

Cracks and Crazes: from molecular simulations to the macroscopic toughness of glassy polymers

Jörg Rottler, Sandra Barsky, and Mark O. Robbins

Department of Physics and Astronomy, The Johns Hopkins University, 3400 N. Charles Street, Baltimore, MD 21218

(February 7, 2020)

We combine molecular dynamics simulations of deformations at the submicron scale with a continuum fracture mechanics calculation for the onset of crack propagation to predict the macroscopic fracture toughness of amorphous glassy polymers. Key ingredients in this multiscale approach are the elastic properties of polymer crazes and the stress at which craze fibrils fail through chain pull-out or scission. Our results are in quantitative agreement with dimensionless ratios that describe experimental polymers and their variation with temperature, polymer length and polymer rigidity.

PACS numbers: 82.35.Lr, 83.60.Uv, 62.20.Mk

Understanding the molecular origins of macroscopic mechanical properties such as the fracture toughness G_c is a fundamental scientific challenge. In tough materials, the work G_c required to propagate a crack through a unit area is orders of magnitude higher than the equilibrium interfacial free energy G_{eq} of the crack surfaces. Efforts to calculate this large toughness enhancement have been frustrated, because phenomena on many length scales must be treated simultaneously [1]. In both amorphous and crystalline materials, the toughness depends on processes that range from breaking of atomic scale bonds to formation of defect structures on micron and larger scales.

In this Letter, we present a multiscale approach that allows us to calculate the toughness enhancement of amorphous polymer glasses. For this important class of materials $G_c/G_{eq} \sim 10^3 - 10^4$, and this large enhancement is essential to their use as adhesives, packaging materials and windows [2–5]. Experiments [5–7] show that the toughness is mainly due to the formation of an intriguing craze structure around the crack tip (Fig. 1). In the craze, $\sim 0.5\text{nm}$ diameter polymers are bundled into an intricate network of $\sim 10\text{nm}$ diameter polymers that extends $\sim 10\mu\text{m}$ on either side of the $\sim \text{mm}$ crack. Molecular level simulations of regions with linear dimensions of mm or even μm are not feasible. They would also be inefficient, since most regions near the crack are homogeneous enough to be treated with continuum mechanics [6,8]. Here, we combine the two approaches using molecular simulations of representative volume elements (see Fig. 1) to provide information about craze formation, deformation and failure that is needed to construct a continuum fracture mechanics model.

One advantage of studying polymeric systems is that many dimensionless ratios are independent of the specific chemistry of the molecules. For this reason we consider a bead-spring model that has been shown to provide a realistic description of polymer behavior [9–12]. Each linear polymer contains N beads of mass m . Van der Waals interactions between beads separated by a distance

r are modeled with a truncated Lennard-Jones potential: $V_{LJ}(r) = 4u_0 [(d/r)^{12} - (d/r)^6 - (d/r_c)^{12} + (d/r_c)^6]$ for $r \leq r_c = 1.5d$, where u_0 and d are characteristic energy and length scales. A simple analytic potential, $V_{br}(r) = -k_1(r - r_c)^3(r - R_1)$, is used for the covalent bonds between adjacent beads along each chain. The constants k_1 and R_1 are adjusted to fit the equilibrium bond length, [9] 0.96σ , and the ratio of the forces at which covalent and van der Waals bonds break. We find that this ratio is the only important parameter in the covalent potential and set it to 100 based on data for real polymers. [12,13] The polymer rigidity and entanglement length N_e are varied by introducing local bond-bending forces [11] with a potential $V_B = \sum_{i=2}^{N-1} b \left(1 - \frac{(\vec{r}_{i-1} - \vec{r}_i) \cdot (\vec{r}_i - \vec{r}_{i+1})}{|\vec{r}_{i-1} - \vec{r}_i| |\vec{r}_i - \vec{r}_{i+1}|} \right)$ along the backbone. \vec{r}_i denotes the position of the i th bead along the chain, and b characterizes the stiffness. Two limiting cases of fully flexible ($N_e \approx 60$ beads, $b = 0u_0$) and semi-flexible ($N_e \approx 30$ beads, $b = 1.5u_0$) chains are considered here. The chainlength is varied from $N = 64$ beads to 1024 beads.

We first show that our model captures the essential experimental features of craze formation (Fig. 1A). The simulation cell has periodic boundary conditions and is initially a cube of size L . The length along one direction L_3 is increased at constant rate, while the other dimensions of the cell are held fixed. Fig. 2(a) shows typical results for the stress σ_3 along the stretching direction as a function of the elongation L_3/L . In all cases, there is an initial peak at small strains, where the material yields by cavitation [14,15]. As in experiment [7], this peak is followed by a long plateau at a constant stress S . During this plateau, deformation is localized in a narrow “active zone” at the boundary of the growing craze network (Fig. 1A). S represents the stress needed to draw fibrils out of the dense regions adjacent to the craze [10]. This steady state drawing process increases the volume occupied by the polymer by a constant factor called the extension ratio λ . When L_3/L reaches λ , the entire system has evolved into a craze, and the stress (Fig. 2(a)) begins to rise.

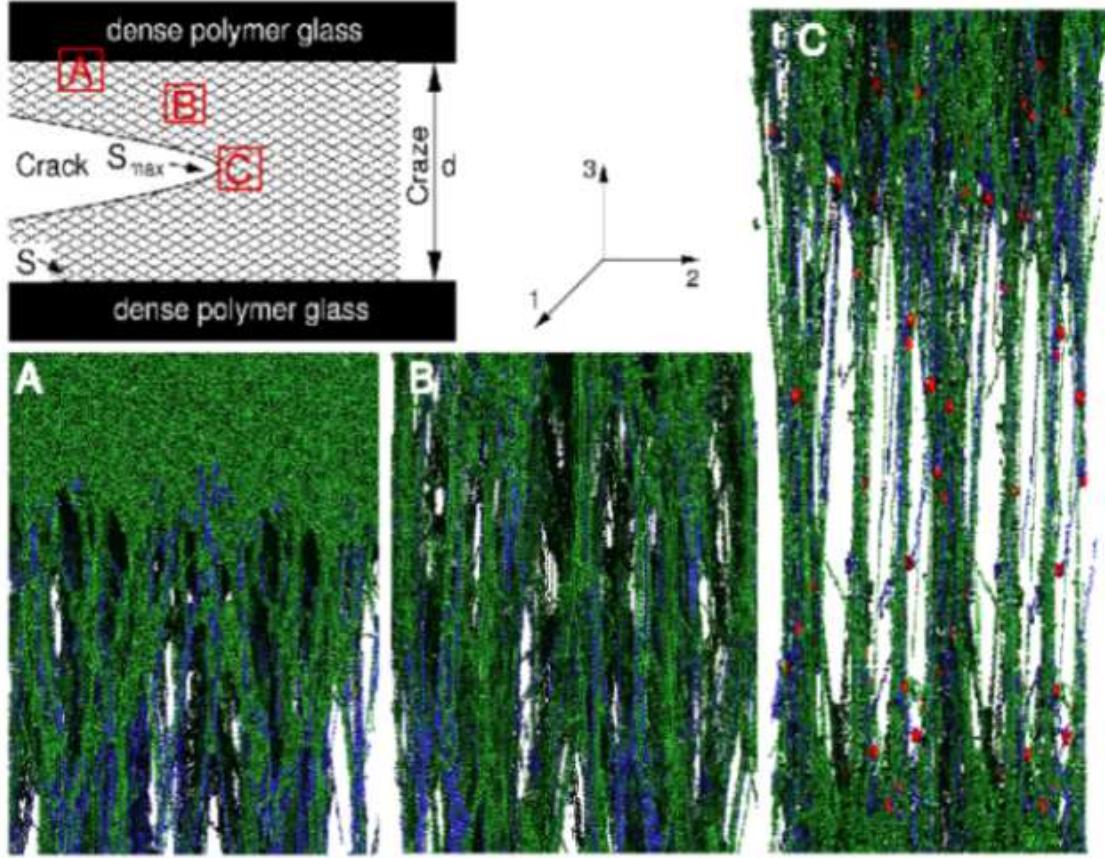


FIG. 1. Length scales involved in the fracture of glassy polymers. A mm-long crack penetrates the material. Ahead of the crack tip a craze zone of typical width $d = 10 - 50 \mu\text{m}$ forms (top left). Craze formation (A), deformation (B) and failure (C) are studied with molecular dynamics simulations of ~ 100 nm-sized volume elements. A: craze fibrils emerge from the dense polymer glass within a narrow “active zone”, B: fully developed craze structure, C: failure of the craze immediately in front of the crack tip. Individual beads of the polymer chains are shown as small ellipsoids. Chains carrying the largest tension are colored blue and broken bonds in Fig C are colored red. The width of each image is 128 bead diameters. The fibril spacing D_0 is ~ 10 bead diameters for this figure, but depends on temperature, chain rigidity and other parameters.

It is evident from Fig. 2(a) that λ is strongly dependent on chain rigidity and thus the entanglement length N_e . We find that λ decreases from about 6.1 for flexible chains to 3.6 for semiflexible chains. As in experiments, these values are quantitatively consistent with a simple model that assumes entanglements act like permanent chemical crosslinks [7]. During crazing, segments between entanglements are expanded from their equilibrium random-walk configurations to nearly straight lines (Fig. 1B).

The dominant contribution to the fracture toughness is the work per unit area needed to form a craze of width d ahead of the crack (Fig. 1). This is equal to the plateau stress S times the increase in width of the polymer from d/λ to d . After normalizing by the lower bound for the toughness provided by the interfacial free energy change $G_{\text{eq}} = 2\gamma$, the toughness enhancement can be written in dimensionless form as

$$\frac{G_c}{G_{\text{eq}}} = \frac{SD_0}{2\gamma} \frac{d}{D_0} (1 - 1/\lambda). \quad (1)$$

This expression shows that G_c is primarily limited by the craze width d . Unlike the other quantities in Eq. (1), d cannot be obtained directly from MD simulations. However, a continuum model proposed by Brown [6] allows us to calculate d .

Brown pointed out that although there is a constant plateau stress S on the craze boundary, a stress concentration occurs near the crack tip (see Fig. 1). He formulated a fracture criterion by equating the stress at the crack tip to the maximum stress S_{max} that the craze fibrils can withstand. The stress at a distance r from a crack tip in a continuous elastic medium diverges as $r^{-1/2}$. This divergence is cut off at the characteristic fibril spacing D_0 , below which the material can no longer be treated as a homogeneous elastic medium. Since the stress varies from S_{max} to S as r varies from D_0 to $d/2$,

$S_{\max} \propto S(d/D_0)^{1/2}$. Solving the complete fracture mechanics problem yields

$$\frac{d}{D_0} = 4\pi\kappa \left(\frac{S_{\max}}{S} \right)^2, \quad (2)$$

where S_{\max} denotes the maximum stress that the craze fibrils can withstand, and the prefactor κ depends on the anisotropic elastic constants c_{ij} of the craze network (Eq. (3)). Neither the elastic properties of the craze network nor S_{\max} are easily obtained from experiments. However, we can calculate both from MD simulations of regions B and C in Fig. 1 and thereby provide the key ingredients for calculating the toughness of glassy polymers from Eqs. (1) and (2).

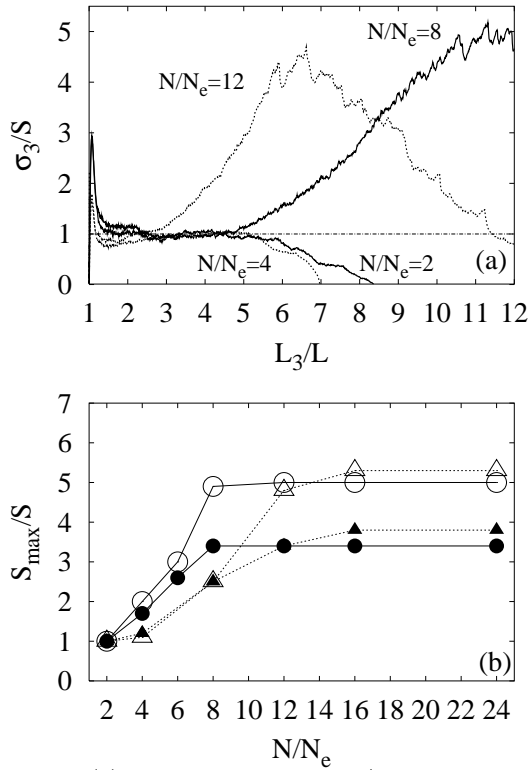


FIG. 2. (a) Normalized stress σ_3/S during craze growth at $T = 0.3 u_0/k_B$ for flexible (solid lines) and semiflexible (dotted lines) chains of the indicated length in systems composed of 32768 beads. Here we take $N_e = 32$ for the semiflexible and $N_e = 64$ for the flexible chains. The value of S_{\max}/S is obtained from the maximum height of the curves. Panel (b) summarizes S_{\max}/S for the flexible (o) as well as semiflexible (\triangle) chains at $T = 0.3 u_0/k_B$ (open symbols) and $T = 0.01 u_0/k_B$ (filled symbols) as a function of chainlength.

Elastic constants were calculated by applying small ($\leq 0.5\%$) step strains to fully developed crazes (Fig. 1B) at two different elongations L_3/L and measuring the change in stress. Table I shows key ratios for flexible and semiflexible chains at two representative temperatures $T = 0.1 u_0/k_B$ and $T = 0.01 u_0/k_B$. Both are well below

the glass transition temperature $T_g \approx 0.35 u_0/k_B$ of the bead-spring model. As can be expected from the highly oriented structure of the craze network (see Fig. 1), c_{33} is always much bigger than the other elastic constants, which are all of the same order. The prefactor κ in Eq. (2) is given by [16]

$$\kappa^2 = \frac{(1 - C_2) + (c_{33}/2c_{44})(1 - C_1)}{2(1 - C_1)^2}, \quad (3)$$

where $C_1 \equiv 2C_2c_{13}/c_{33}$ and $C_2 \equiv c_{13}/(c_{11} + c_{12})$. Inserting the elastic constants, we obtain values for κ between 2.0 and 2.8 for flexible chains and between 1.1 and 1.7 for semiflexible chains. The crazes with higher elongations always have a lower value of κ .

A simple approximate expression $\kappa \approx \sqrt{c_{33}/4c_{44}}$ can be obtained by noting that $c_{33} \gg c_{13}$, and thus $C_1 \sim 0$ and $C_2 \sim 1$. Table I also shows that this is an accurate approximation for all practical purposes. This simple expression shows clearly that the ability of crazes to resist shear ($c_{44} > 0$) limits their toughness. As first pointed out by Brown [6], the absence of lateral stress transfer would lead to $\kappa \rightarrow \infty$ and thus to an infinite toughness.

To determine the stress S_{\max} at which fibrils break, we continue straining the fully developed craze until it fails (Fig. 1C). Although all chains that are long enough to form stable crazes ($N/N_e \geq 2$ [10]) show the same plateau stress and extension ratio, their crazes exhibit very different behavior for $L_3/L > \lambda$ (Fig. 2(a)). Short chains of length $N/N_e = 2$ easily pull free from the topological constraints imposed by entanglements, and the stress drops monotonically. As N increases, the force needed to pull chains free from entanglements along a failure plane rises, and there is a corresponding increase in S_{\max} . The failure mechanism changes when the force needed to disentangle the chains reaches the breaking force for covalent bonds. At this point the forces along the chains and S_{\max} both saturate due to chain scission.

Fig. 2(b) summarizes our results for S_{\max}/S as a function of chain length, temperature and flexibility. As N/N_e rises above 2, S_{\max}/S rises rapidly and then saturates due to the change in failure mechanism from chain pullout to chain scission. Saturation occurs for N/N_e between 6 and 8 for flexible chains and between 12 and 16 for semiflexible chains with $f_b/f_{LJ} = 100$. The limiting value of S_{\max}/S lies between 3.4-3.8 for $T = 0.01 u_0/k_B$ and 5.0-5.3 for $T = 0.3 u_0/k_B$ and increases slightly with chain rigidity. In general, more chain scission is observed for chains with higher rigidity and at lower temperatures.

We are now in a position to evaluate Eq. (2) and compare our results to experimental values. Taking $\kappa = 2.0 - 2.8$ for flexible chains and $S_{\max}/S = 3.4 - 5.0$, we predict a dimensionless ratio of d/D_0 between 290 - 890. Semiflexible chains give d/D_0 between 200 - 600. Typical craze widths d observed in experiments range between 3 - 20 μm , whereas characteristic fibril spacings

D_0 have values between 20 – 30 nm. Thus the range of experimental values for $d/D_0 = 100 - 1000$ overlaps well with our predictions.

In addition to values quoted above, calculating the toughness enhancement from Eq. (1) requires values for the plateau stress S , the mean fibril spacing D_0 , and the surface tension γ . Typical values from our simulations are $S = 0.5 - 1.4 u_0/d^3$, $D_0 = 10 - 14 d$, and $\gamma = 0.6 - 1.0 u_0/d^2$. With these values, we arrive at our final result $G_c/G_{eq} = 1300 - 4300$ (flexible polymers) and $G_c/G_{eq} = 1200 - 3500$ (semiflexible polymers). Within this range, G_c/G_{eq} tends to drop with increasing chain rigidity and decreasing temperature T . This trend is also found in real adhesive joints, where the toughness generally decreases with decreasing temperature [2].

Our simulations agree with experimental observations in greater detail. Sha *et. al.* [17] have compiled values of G_c for polystyrene (PS) and polymethylmethacrylate (PMMA) as a function of polymer molecular weight M_n . Neither polymer shows a toughness enhancement when M_n is less than twice M_e . As in our simulations (Fig. 3), the toughness rises rapidly as M_n/M_e rises above 2 and then saturates between 5 and 10 M_e . The limiting toughness enhancements take on values of about 2500 (PMMA) and 5000 (PS) that are comparable to our predicted values.

In conclusion, we have demonstrated that supplementing a continuum model with constitutive relations from molecular simulations can provide quantitative predictions for key material parameters such as the fracture toughness. This approach can be further developed by using chemically detailed interaction potentials for specific polymers in the molecular simulations. A more detailed finite element model for crack propagation could also be used, as in recent work [18,19] that assumed simple constitutive relations for craze widening and breakdown. Although one might hope to include all length scales simultaneously in a hybrid calculation, this is complicated by the rapid increase in the relevant time scale with increasing length scale [8].

This work was supported by the Semiconductor Research Corporation (SRC) and the National Science Foundation (NSF grant No. 0083286). We thank H. R. Brown, E. J. Kramer, and C. Denniston for stimulating discussions.

- [3] A. V. Pocius, *Adhesion and adhesives technology: an introduction*, (Hanser/Gardner, Munich, 1997).
- [4] R. A. L. Jones, R. W. Richards, *Polymers at Surfaces and Interfaces*, (Cambridge University Press, Cambridge, 1999).
- [5] R. N. Haward, R. J. Young, Eds., *The Physics of Glassy Polymers*, (Chapman & Hall, London, 1997).
- [6] H. R. Brown, *Macromolecules* **24**, 2752 (1990).
- [7] E. J. Kramer, L. L. Berger, *Adv. Polymer Science* **91/92**, 1 (1990).
- [8] F. F. Abraham, J. Q. Broughton, N. Bernstein, E. Kaxiras, *Europhys. Lett.* **44**, 783 (1998); J. Q. Broughton, F. F. Abraham, N. Bernstein, E. Kaxiras, *Phys. Rev. B* **60**, 2391 (1999).
- [9] M. Pütz, K. Kremer, G. S. Grest, *Euro. Phys. Lett.* **49**, 735 (2000).
- [10] A. R. C. Baljon, M. O. Robbins, *Macromolecules* **34**, 4200 (2001).
- [11] R. Faller, F. Müller-Plathe, and A. Heuer, *Macromolecules* **33**, 6602 (2000) and R. Faller and F. Müller-Plathe, *ChemPhysChem* **2**, 180 (2001).
- [12] S. W. Sides, G. S. Grest, M. J. Stevens, *Phys. Rev. E* **64**, 050802 (2001).
- [13] M. J. Stevens, *Macromolecules* **34**, 1411 (2001); *Macromolecules* **34**, 2710 (2001).
- [14] J. Rottler, M. O. Robbins, *Phys. Rev. E* **64**, 051801 (2001).
- [15] A. R. C. Baljon, M. O. Robbins, *Science* **271**, 482 (1996).
- [16] P. C. Paris, G. C. Sih, *Fracture Toughness Testing and its Applications*, American Society for Testing and Materials, Philadelphia, PA.
- [17] Y. Sha, C. Y. Hui, A. Ruina, E. J. Kramer, *Macromolecules* **28**, 2450 (1995).
- [18] M. G. A. Tijssens, E. van der Giessen, L. J. Sluys, *Mechanics of Materials* **32**, 19 (2000); R. Estevez, M. G. A. Tijssens, E. van der Giessen, *J. Mech. and Physics of Solids* **48**, 2585 (2000); M. G. A. Tijssens, E. van der Giessen, L. J. Sluys, *Int. J. of Solids and Structures* **37**, 7307 (2000).
- [19] S. Socrate, M. C. Boyce, A. Lazzeri, *Mech. Mater.* **33**, 155 (2001).

TABLE I. Elastic properties of model crazes composed of 262 144 beads with flexible (fl.) and semiflexible (sfl.) chains at two elongations L_3/L . Uncertainties in c_{ij} are about 10%. Here $N = 256$, but the results do not depend on N for $N > 2N_e$. They are also insensitive to the covalent bond potential, since strain is accommodated by the weaker van der Waals bonds.

	$T[u_0/k_B]$	L_3/L	c_{11}/c_{33}	c_{44}/c_{33}	κ	$\sqrt{c_{33}/4c_{44}}$
fl.	0.01	5.5	0.026	0.038	2.8	2.6
	0.01	7.9	0.016	0.065	2.0	2.0
	0.1	5.8	0.030	0.041	2.7	2.5
	0.1	7.9	0.015	0.054	2.2	2.1
sfl.	0.01	3.4	0.12	0.10	1.7	1.6
	0.01	4.8	0.051	0.10	1.6	1.6
	0.1	3.4	0.087	0.086	1.9	1.7
	0.1	4.8	0.026	0.15	1.4	1.3

[1] *Materials Research by Means of Multiscale Computer Simulation*, MRS Bulletin **26**, No. 3 (2001)

[2] R. P. Wool, *Polymer Interfaces: Structure and Strength*, (Hanser/Gardner, Munich, 1995).